DNA damage response mutations enhance the antitumor efficacy of ATR and PARP inhibitors in cholangiocarcinoma cell lines

TASSANEE LERKSUTHIRAT[1], SUNISA PRASOPPORN[2], RAKKREAT WIKINIYADHANEE[3], SERMSIRI CHITPHUK[1], WASANA STITCHANTRAKUL[1], PARAVEE OWNEIUM[3], SIWANON JIRAWATNOTAI[2] and DONNIPHAT DEJSUPHONG[3]

[1]Research Center, Faculty of Medicine Ramathibodi Hospital, Mahidol University, Bangkok 10400, Thailand; [2]Siriraj Center of Research for Excellence (SiCORE) for Systems Pharmacology, Department of Pharmacology, Faculty of Medicine Siriraj Hospital, Mahidol University, Bangkok 10700, Thailand; [3]Program in Translational Medicine, Chakri Naruebodindra Medical Institute, Faculty of Medicine Ramathibodi Hospital, Mahidol University, Samutprakarn 10540, Thailand

Received July 3, 2024; Accepted November 28, 2024

DOI: 10.3892/ol.2025.14874

Abstract. Cholangiocarcinoma (CCA) is a biliary tract carcinoma that is challenging to treat due to its heterogeneity and limited treatment options. Genetic alterations in DNA damage response (DDR) pathways and homologous recombination (HR) defects are common in CCA. This has prompted interest in the use of ataxia telangiectasia and Rad3-related protein (ATR) and poly(ADP-ribose) polymerase (PARP) inhibitors to treat CCA. The present study investigated the impact of an ATR inhibitor and various PARP inhibitors, individually and in combination, on CCA cell lines with different DDR mutation profiles. DDR gene alterations in these cell lines were analyzed, and the responses of the cells to treatment with the PARP inhibitors olaparib, veliparib and talazoparib and/or the ATR inhibitor AZD6738 were evaluated. Assessments focused on cellular viability, clonogenic survival and the combination index, alongside changes in DNA damage assessed via the formation of micronuclei and γ-H2A histone family member X foci. The results revealed that the CCA cell lines with more DDR mutations exhibited greater sensitivity to single and combination treatments. Talazoparib was found to be the most potent PARP inhibitor in the CCA cell lines. The combination of AZD6738 and talazoparib demonstrated varying synergistic effects depending on the genetic background of the CCA cells, with greater efficacy in the cell lines less sensitive to single drug treatments. Mechanistically, this combination promoted the accumulation of DNA damage, including DNA double-strand breaks. Overall, the study underscores the importance of HR in CCA. It reveals an association between the extent of DDR mutations and the response to AZD6738 and PARP inhibitors in CCA, both as single agents and in combination. These findings highlight that the number of mutated genes influences variability in the drug response.

Correspondence to: Dr Siwanon Jirawatnotai, Siriraj Center of Research for Excellence (SiCORE) for Systems Pharmacology, Department of Pharmacology, Faculty of Medicine Siriraj Hospital, Mahidol University, 2 Wanglang Road, Bangkoknoi, Bangkok 10700, Thailand
E-mail: siwanon.jir@mahidol.ac.th

Dr Donniphat Dejsuphong, Program in Translational Medicine, Chakri Naruebodindra Medical Institute, Faculty of Medicine Ramathibodi Hospital, Mahidol University, 111 Suwannabhumi Canal Road, Bang Pla, Bang Phli District, Samutprakarn 10540, Thailand
E-mail: donniphat.dej@mahidol.ac.th

Key words: biliary tract cancer, cholangiocarcinoma, ATR inhibitor, PARP inhibitor, drug combination, combination index, DNA damage response

Introduction

Cholangiocarcinoma (CCA) is one of the most challenging carcinomas to manage, given its inherent heterogeneity and the limited efficacy of available therapeutic options. Epidemiological data reveals that CCA constitutes ~15% of primary liver cancers and ~3% of gastrointestinal malignancies, contributing to nearly 2% of all annual cancer-associated fatalities globally (1,2). Most patients present with advanced CCA, as the early stages are typically asymptomatic. Modern radiographic diagnostic techniques, including abdominal magnetic resonance imaging, abdominal computerized tomography and magnetic resonance cholangiopancreatography, are able to detect CCA. However, these techniques generally require verification via histological or cytological analysis.

Depending on the characteristics of the CCA, neoadjuvant chemotherapy may be used to reduce the size of large tumors prior to surgery (3). If the tumor is considered to be resectable, surgical resection is typically the initial approach, followed by adjuvant chemotherapy to reduce the risk of recurrence (2). In cases where surgical removal is not feasible, palliative chemotherapy can be administered to improve the quality of life of the patient. Currently, patients with CCA are treated with conventional DNA-damaging chemotherapies. These

include platinum-based drugs such as cisplatin, gemcitabine, oxaliplatin and capecitabine, in addition to a combination of 5-fluorouracil and folinic acid (4,5). However, it is necessary to improve the efficacy of these treatments, as CCA can develop resistance and become unresponsive to chemotherapy.

In the age of personalized medicine, the molecular profiling of CCA facilitates the use of targeted treatments (6,7). This approach leverages the concept of synthetic lethality, in which the concurrent inhibition of two associated genes results in cell death (8). Notably, the DNA damage and repair pathways have been identified as promising targets for the inhibition of cancer growth (9). Poly(ADP-ribose) polymerase (PARP), an enzyme involved in DNA repair, exhibits synthetic lethality with breast and ovarian cancer susceptibility protein 1/2 (BRCA1/2), which is key to homologous recombination (HR) repair (10). Targeting PARP in tumors with a defective *BRCA1/2* gene causes the accumulation of DNA damage and subsequently induces cell death. The US Food and Drug Administration (FDA) has approved numerous PARP inhibitors, including olaparib (11), rucaparib (12) and niraparib (13) and talazoparib (14), whereas fluzoparib (15) and pamiparib (16) were approved in China. Ataxia telangiectasia and Rad3-related protein (ATR) serves as a DNA damage sensor and plays a crucial role in the response to replicative stress (17). A functional loss of ATR can sensitize cancer cells to DNA-damaging chemotherapeutics, while ATR activation contributes to the development of resistance to PARP inhibitors via the mitigation of replicative stress (10). Notably, ATR has been reported to exhibit synthetic lethality with PARP (17,18), and currently, at least eight ATR inhibitors are undergoing clinical trials (19). Efforts to combine ATR inhibitors with PARP inhibitors are ongoing, with the aim of overcoming resistance, enhancing therapeutic effectiveness, and potentially reducing the dosage of each drug, thereby decreasing toxicity.

A number of clinical trials have explored the combined use of ATR and PARP inhibitors in the treatment of ovarian cancer (20), breast cancer (21) and prostate cancer (22). In the context of CCA, one such trial is currently suspended (23), while another is evaluating the combination of the ATR inhibitor AZD6738 with the PARP inhibitor olaparib (24). Several *in vitro*, *in vivo*, and *ex vivo* studies have investigated the effects of PARP or ATR inhibitors, and their combinations with DNA-damaging agents on CCA (25-27). For example, Serra-Camprubí *et al* (25) assessed the effects of the PARP inhibitors olaparib, pamiparib and niraparib on patient-derived xenograft (PDX) cell lines from patients with CCA and diverse genetic profiles. The study concluded that patients with advanced CCA and pathogenic *BRCA2* mutations could potentially benefit from PARP inhibitor treatment. Similarly, Bezrookove *et al* (26) evaluated the impact of olaparib and niraparib on PDX and established CCA cell lines, all with various DNA damage repair gene mutation profiles. The study showed that niraparib was more potent than olaparib, and the combination of niraparib with gemcitabine synergistically inhibited tumor growth. Additionally, Moolmuang and Ruchirawat (27) investigated the cytotoxic effects of the ATR inhibitor VE-821, both alone and in combination with the ATM serine/threonine kinase inhibitor KU-55933, on various CCA cell lines. The combination of the two inhibitors had a greater effect on growth inhibition than either inhibitor alone in all the cell lines tested. However, research on the effects of combining ATR with different PARP inhibitors on CCA cell lines is limited (28).

In the present study, the aim was to investigate the effects of various PARP inhibitors, namely, olaparib, veliparib and talazoparib, and the ATR inhibitor AZD6738, both individually and in combination, on established cell lines with diverse genetic backgrounds. Additionally, the mechanism of the DNA damage response (DDR) elicited by these treatments was examined, and the synergistic activity between AZD6738 and the various PARP inhibitors was assessed to determine their efficacy via the combination index (CI).

Materials and methods

Drugs. Olaparib (cat. no. HY-10162), veliparib (cat. no. HY-10129), talazoparib (cat. no. HY-16106) and AZD6738 (cat. no. HY-19323) were purchased from MedChemExpress. Olaparib and veliparib were dissolved in 100% dimethyl sulfoxide (DMSO; cat. no. A3672,0250; PanReac AppliChem; ITW Reagents Division) to create a 100 mM stock solution, while talazoparib and AZD6738 were dissolved in DMSO to a concentration of 50 mM. The drug stocks were kept at -80˚C until used.

Cell lines and culture. The MMNK-1 (cat. no. JCRB1554; immortalized human cholangiocyte) (29) and HuH-28 (cat. no. JCRB0426; cholangiocarcinoma) (30) cell lines were obtained from the Japanese Collection of Research Bioresources Cell Bank (JCRB), while the TFK-1 (cell no. RCB2537; cholangiocarcinoma) cell line (31) was received from the RIKEN BioResource Center. SiSP-K01 and SiSP-K05 primary cell lines were a gift from Professor Seiji Okada of Kumamoto University (Kumamoto, Japan) (32). SiSP-K01 was derived from a 64-year-old female with intrahepatic, moderately differentiated CCA and was used at passage 51. SiSP-K05 was derived from another female patient, age 53 years, with intrahepatic, moderately differentiated CCA and was also used at passage 51. The origin of each cell line is summarized in Table SI. The experimental protocol was approved by the Human Research Ethics Committee of the Faculty of Medicine, Ramathibodi Hospital, Mahidol University (Bangkok, Thailand; approval no. MURA2023/155).

The MMNK-1 and TFK-1 cell lines were maintained in DMEM/F12 (cat. no. 12400024; Gibco; Thermo Fisher Scientific, Inc.) and RPMI-1640 medium (cat. no. 11875093; Gibco; Thermo Fisher Scientific, Inc.), respectively. The HuH-28, SiSP-K01 and SiSP-K05 cell lines were cultured in DMEM (cat. no. 12800017; Gibco; Thermo Fisher Scientific, Inc.). All cell lines were supplemented with 1% penicillin/streptomycin (cat. no. 15140122; Invitrogen; Thermo Fisher Scientific, Inc.) and 10% fetal bovine serum (FBS; cat. no. ES-009-B; Merck KGaA), with the exception of MMNK-1, which was supplemented with 15% FBS. The cells were incubated at 37˚C with 5% CO_2.

Mutation analysis of CCA cell lines. The genetic profiles of the TFK-1 and HuH-28 cell lines were obtained by next-generation sequencing, as described in Jamnongsong *et al* (33). The genetic profiles of SiSP-K01 (https://www.ncbi.nlm.

nih.gov/sra/SRR31111387), and SiSP-K05 (https://www.ncbi.nlm.nih.gov/sra/SRR31111386) were also obtained by next-generation sequencing and are available under BioProject ID PRJNA1176211 (https://www.ncbi.nlm.nih.gov/bioproject/PRJNA1176211/). The set of 27 DDR genes was based on those in the study by Bezrookove *et al* (26); AT-rich interaction domain 1A/B (*ARID1A* and *ARID1B*), ataxia telangiectasia mutated (*ATM*), *ATR*, ATRX chromatin remodeler (*ATRX*), BRCA1 associated deubiquitinase 1 (*BAP1*), BRCA1 associated RING domain 1 (*BARD1*), BLM RecQ like helicase (*BLM*), *BRCA1*, *BRCA2*, BRCA1 interacting DNA helicase 1 (*BRIP1*), checkpoint kinase 2 (*CHEK2*), FA complementation group A/C/D2/E/F/G/L (*FANCA*, *FANCC*, *FANCD2*, *FANCE*, *FANCF*, *FANCG* and *FANCL*), MRE11 homolog, double strand break repair nuclease (*MRE11*), nibrin (*NBN*), partner and localizer of BRCA2 (*PALB2*), RAD50 double strand break repair (*RAD50*), RAD51 recombinase (*RAD51*), RAD51 paralog B/C (*RAD51B* and *RAD51C*) and WRN RecQ like helicase (*WRN*). To assess the pathogenicity of the identified exonic mutations that led to changes in amino acids, the Franklin tool by Genoox (http://franklin.genoox.com; accessed on September 26, 2023) was employed. This analysis was conducted in accordance with the Association for Molecular Pathology (AMP) classification guidelines. These guidelines stratify variants into four tiers based on their clinical relevance to bile duct cancer, as discussed by Li *et al* (34). Tier 1 includes variants with strong clinical significance, tier 2 comprises variants with potential significance, tier 3 encompasses variants of uncertain significance, and tier 4 contains variants that are benign or likely to be benign.

Sensitivity assay and CI calculation. Cells were seeded into 96-well plates at a final concentration of 3,000 cells/well and incubated for 24 h before the medium was replaced with that containing the drugs of interest. Treatments were with either a PARP inhibitor (olaparib, veliparib, and talazoparib) or the ATR inhibitor AZD6738 alone, or a combination of PARP inhibitor and AZD6738, for a duration of 120 h at 37˚C. A mock treatment was also conducted, in which the concentration of DMSO was >0.016%. Following treatment, cell viability was assessed using the CellTiter-Glo® Luminescent Cell Viability Assay according to the manufacturer's protocol (cat. no. G7572; Promega Corporation). Survival percentages were determined by normalizing the luminescent signal to that of untreated cells. These percentages were then plotted and half maximal inhibitory concentration (IC_{50}) values were calculated using GraphPad Prism software, version 9.5.1 (Dotmatics). The CI values were subsequently calculated according to the Chou-Talalay method (35) as shown below:

$$CI = \frac{(IC_{50c})_1}{(IC_{50a})_1} + \frac{(IC_{50c})_2}{(IC_{50a})_2}$$

In this formula, $(IC_{50c})_1$ is the IC_{50} of AZD6738 used in combination; $(IC_{50a})_1$ is the IC_{50} of AZD6738 used alone; $(IC_{50c})_2$ is the IC_{50} of the PARP inhibitor used in combination and $(IC_{50a})_2$ is the IC_{50} of the PARP inhibitor used alone.

The CI values were categorized as follows (36): 0.1-0.3, strong synergism; 0.3-0.7, synergism; 0.7-0.85, moderate synergism; 0.85-0.9, slight synergism; 0.9-1.1, nearly additive; 1.1-1.2, slight antagonism; 1.2-1.45, moderate antagonism. The experiments were conducted in three biological replicates.

Clonogenic survival assays. Cells were seeded in 6-well plates at a density of 600 cells/well for MMNK-1 or 1,000 cells/well for SiSP-K01 and SiSP-K05 and incubated at 37˚C with 5% CO_2 for 24 h. They were then exposed to AZD6738, various concentrations of PARP inhibitors, or a combination of both, for 120 h at 37˚C. The media was subsequently replaced, and the cells were incubated for 7-10 days until colonies formed. For visualization, a 0.5% w/v solution of crystal violet (cat. no. C077; Sigma-Aldrich; Merck KGaA) in 40% v/v methanol in water was added and incubated for 10 min at room temperature. The plates were then washed and air-dried, and images were acquired using a ChemiDoc™ MP Imaging System (Bio-Rad Laboratories, Inc.). All the images were exported as tif files, and the intensity of each well was measured using ImageJ 1.53n software (37) as previously described (38). The experiments were performed on three biological replicates.

Micronuclei and γ-H2A histone family member X (γ-H2AX) foci formation assays. Cells were seeded in a slide chamber (Lab-Tek™, cat. no. 154526; Thermo Fisher Scientific, Inc.) and allowed to grow until they reached 80% confluence. Subsequently, the medium was replaced with fresh media containing AZD6738, PARP inhibitor or a combination of AZD6738 and PARP inhibitor. The cells were then incubated for an additional 24 h at 37˚C in a 5% CO_2 atmosphere. Fluorescence staining was performed using a method modified from that in previous studies (39,40). Briefly, cells were washed with PBS and fixed with 4% paraformaldehyde for 10 min at room temperature. After another wash with PBS, cells were permeabilized with 0.5% Triton X-100 in PBS for 15 min. Non-specific binding was blocked using Intercept® (PBS) blocking buffer (cat. no. 927-70001; LI-COR Biosciences) for 1 h at room temperature. For the detection of γ-H2AX foci, cells were incubated with a mouse monoclonal antibody against γ-H2AX (Ser139; 1:1,000; cat. no. 80312; Cell Signaling Technology, Inc.) at 4˚C overnight. Alexa Fluor® 488 donkey anti-mouse IgG (1:500; cat. no. A21202; Thermo Fisher Scientific, Inc.) was used as the secondary antibody and was incubated with the cells for 1 h at room temperature. Micronuclei and nuclei were visualized with Hoechst 33342 solution (1:2,000; cat. no. H3570; Thermo Fisher Scientific, Inc.) for 5 min at room temperature. Images were acquired with a fluorescence microscope (ECLIPSE Ci; Nikon Corporation). All samples were visualized using the same intensity and exposure time, and images were analyzed using ImageJ 1.53n software (37). At least 225 nuclei were analyzed for both micronuclei and γ-H2AX foci formation. The experiments were performed with at least two biological replicates.

Statistical analysis. The IC_{50} and CI results were reported as the mean ± standard deviation. The IC_{50} values and relative intensities of colonies across each CCA cell line were statistically compared with those of the MMNK-1 cholangiocyte cell line, utilizing multiple t-tests with the Holm-Sidak method in GraphPad Prism software, version 9.5.1 (Dotmatics). $P<0.05$

was considered to indicate a statistically significant difference. The same statistical analysis was applied to assess significant differences in the average number of micronuclei per cell between treatments with AZD6738 or PARP inhibitors alone or in combination. The results of the γ-H2AX foci formation assay are presented as medians and were analyzed using the Mann-Whitney test.

Results

Genetic profiling of DDR in CCA cell lines and AMP classification. As shown in Table I, the numbers of mutated genes differed among the CCA cell lines. Among the four CCA cell lines, TFK-1 had the fewest DDR mutated genes (n=9), whereas HuH-28 had the same number of DDR mutated genes as SiSP-K01 (n=11). SiSP-K05 contained the highest number of mutated genes (n=15). Fig. 1 demonstrates the distribution of DDR mutated genes in each CCA cell line. In all CCA cell lines analyzed, mutations in *ATR*, *BRCA2* and *WRN* were detected. In addition, a subset of three CCA cell lines exhibited mutations in eight different genes: *ARID1A*, *ARID1B*, *ATM*, *ATRX*, *BARD1*, *BRIP1*, *FANCA* and *PALB2*. Three other mutated genes, *BLM*, *BRCA1* and *RAD51B*, were found in two CCA cell lines; HuH-28 and SiSP-K05 for *BLM* and *BRCA1*, and *RAD51B* for SiSP-K01 and SiSP-K05. There were four mutated genes, namely *BAP1*, *CHEK2*, *FANCF* and *RAD50,* that were only observed in a single CCA cell line. However, there were nine genes associated with DDR, specifically *FANCC*, *FANCD2*, *FANCE*, *FANCG*, *FANCL*, *MRE11*, *NBN*, *RAD51* and *RAD51C,* that were not detected in any of the CCA cell lines. Details of the genetic variants in DDR genes that were identified are presented in Table SII. Next, the classification of genetic variants in DDR genes was determined according to the guidelines of the AMP, as indicated in Table II. SiSP-K01 exhibited a range of variants spanning the clinically relevant tiers 2-4, whereas SiSP-K05 had a range of variants spanning tiers 2 and 3. Notably, the TFK-1 and HuH-28 cell lines only demonstrated variants exclusively from tiers 3 and 4. Additionally, it was observed that variants in *BRCA1* and *PALB2* genes were confined to tiers 2 and 3, whereas those in the *BRCA2* and *BRIP1* genes spanned tiers 2-4. Variants in other genes fell into tier 3 and/or tier 4. Collectively, these findings suggest that the CCA cell lines are promising candidates for further testing with PARP inhibitors and AZD6738.

Evaluating the impacts of AZD6738 and PARP inhibitors on cell viability and clonogenic survival. To assess cell viability in the four CCA cell lines with distinct DDR mutated backgrounds, TFK-1, HuH-28, SiSP-K01 and SiSP-K05 cells were treated with AZD6738, PARP inhibitors alone, or their combinations, and their responses to treatment were compared with those of the immortalized cholangiocyte cell line MMNK-1. Fig. 2 and Table III display the dose-response curves from the sensitivity assay and the IC_{50a} profiles of all the cell lines in response to AZD6738 and the various PARP inhibitors, respectively.

Comparison of AZD6738 and the PARP inhibitors indicated that AZD6738 was the most toxic to the cell lines. This is evidenced by AZD6738 having the lowest IC_{50a} values, both minimal and maximal, in comparison with the PARP inhibitors. The IC_{50a} values for AZD6738 ranged from 0.554±0.020 μM (in SiSP-K05) to 15.633±5.324 μM (in SiSP-K01). By contrast, the ranges of the IC_{50a} values for the PARP inhibitors were as follows: Olaparib, from 19.740±16.283 μM (in HuH-28) to 121.067±5.140 μM (in SiSP-K01); veliparib, from 67.607±3.466 μM (in SiSP-K05) to 256.800±14.127 μM (in MMNK-1); and talazoparib, from 1.095±0.920 μM (in HuH-28) to 127.767±39.302 μM (in MMNK-1).

Next, the IC_{50a} profiles of CCA cell lines when treated with AZD6738 or various PARP inhibitors alone were compared with those of MMNK-1 cholangiocytes (Table III). For AZD6738, only SiSP-K05 (IC_{50a}, 0.554±0.020 μM) was significantly more sensitive (P=0.017) than the MMNK-1 cholangiocytes (IC_{50a}, 0.997±0.141 μM). By contrast, SiSP-K01 cells (IC_{50a}, 15.633±5.324 μM; P=0.018) exhibited significantly lower sensitivity than MMNK-1 cholangiocytes to AZD6738, while TFK-1 and HuH-28 cells both displayed sensitivity levels similar to those of the cholangiocytes. For the PARP inhibitors, three CCA cell lines, namely TFK-1 (IC_{50a}, 25.667±3.661 μM; P<0.001), HuH-28 (IC_{50a}, 19.740±16.283 μM; P=0.010) and SiSP-K05 (IC_{50a}, 46.790±16.939 μM; P=0.021), demonstrated significantly greater sensitivity than MMNK-1 cells (IC_{50a}, 85.033±5.664 μM) to olaparib, while HuH-28 (IC_{50a}, 145.950±10.112 μM; P=0.010), SiSP-K01 (IC_{50a}, 143.833±20.857 μM; P=0.005) and SiSP-K05 cells (IC_{50a}, 67.607±3.466 μM; P<0.001) were significantly more sensitive than MMNK-1 cells (IC_{50a}, 256.800±14.127 μM) to veliparib. Additionally, the sensitivity of HuH-28 and SiSP-K05 cells to talazoparib was heightened compared with that of MMNK-1 cells. SiSP-K01 cells (IC_{50a}, 121.067±5.140 μM; P=0.005) were significantly less sensitive than MMNK-1 cells to olaparib, whereas TFK-1 cells displayed veliparib sensitivity comparable to that of MMNK-1 cells. The sensitivity to talazoparib of TFK-1 and SiSP-K01 cells was similar to that of MNNK-1 cells. Among the cell lines with significantly greater sensitivity than MNNK-1 cells to PARP inhibitors, talazoparib was the most potent, as evidenced by its low IC_{50a}. The IC_{50a} values for the PARP inhibitors were as follows: Olaparib, MMNK-1 (85.033±5.664 μM) compared with TFK-1 (25.667±3.661 μM), HuH-28 (19.740±16.283 μM) and SiSP-K05 (46.790±16.939 μM); veliparib, MMNK-1 (256.800±14.127 μM) compared with HuH-28 (145.950±10.112 μM), SiSP-K01 (143.833±20.857 μM) and SiSP-K05 (67.607±3.466 μM); and talazoparib, MMNK-1 (127.767±39.302 μM) compared with HuH-28 (1.095±0.920 μM) and SiSP-K05 (4.378±1.977 μM).

The clonogenicity of the two primary CCA cell lines and MMNK-1 cholangiocytes when treated individually with AZD6738 and of PARP inhibitors at the respective IC_{50a} was evaluated (Fig. S1). The results demonstrate that all inhibitors inhibited clonogenicity. The inhibitory effect on clonogenic survival was >50% when compared with the clonogenicity of the untreated group. These results confirm that at the IC_{50a}, these drugs are capable of inhibiting the clonogenicity of primary cell lines.

Collectively, these observations suggest that, compared with AZD6738, PARP inhibitors exhibit a broader range of effectiveness in CCA cell lines with diverse genetic backgrounds and less toxicity. Among the tested PARP inhibitors, talazoparib is the most potent.

Table I. List of DDR mutated genes in CCA cell lines.

CCA cell lines	DDR mutated genes
TFK-1	*ATM, ATR, BAP1, BARD1, BRCA2, BRIP1, FANCA, PALB2, WRN*
HuH-28	*ARID1A, ARID1B, ATM, ATR, ATRX, BARD1, BLM, BRCA2, BRIP1, FANCA, WRN*
SiSP-K01	*ARID1A, ARID1B, ATM, ATR, ATRX, BARD1, BRCA1, BRCA2, PALB2, RAD51B, WRN*
SiSP-K05	*ARID1A, ARID1B, ATR, ATRX, BLM, BRCA1, BRCA2, BRIP1, CHEK2, FANCA, FANCF, PALB2, RAD50, RAD51B, WRN*

ARID1A/B, AT-rich interaction domain 1A/B; ATM, ataxia telangiectasia mutated; ATR, ataxia telangiectasia and Rad3-related protein; ATRX, ATRX chromatin remodeler; BAP1, BRCA1 associated deubiquitinase 1; BARD1, BRCA1 associated RING domain 1; BLM, BLM RecQ like helicase; BRIP1, BRCA1 interacting DNA helicase 1; CCA, cholangiocarcinoma; CHEK2, checkpoint kinase 2; DDR, DNA damage response; FANCA/F, FA complementation group A/F; PALB2, partner and localizer of BRCA2; RAD50, RAD50 double strand break repair; RAD51B, RAD51 recombinase paralog B; WRN, WRN RecQ like helicase.

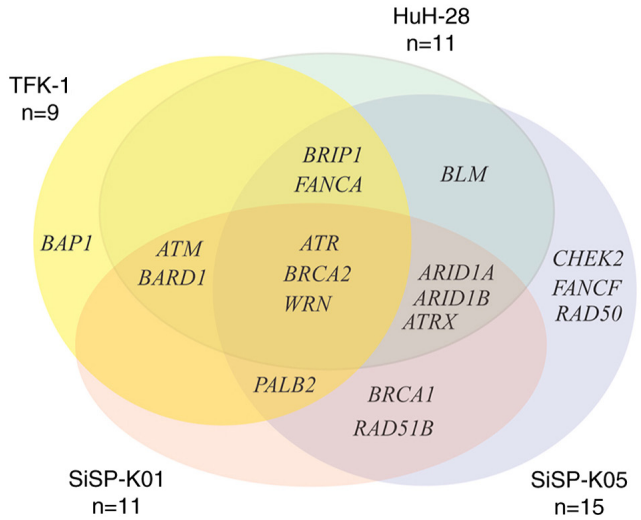

Figure 1. Venn diagram of mutated DNA damage response genes in cholangiocarcinoma cell lines. ARID1A/B, AT-rich interaction domain 1A/B; ATM, ataxia telangiectasia mutated; ATR, ataxia telangiectasia and Rad3-related protein; ATRX, ATRX chromatin remodeler; BAP1, BRCA1 associated deubiquitinase 1; BARD1, BRCA1 associated RING domain 1; BLM, BLM RecQ like helicase; BRIP1, BRCA1 interacting DNA helicase 1; CHEK2, checkpoint kinase 2; FANCA/F, FA complementation group A/F; PALB2, partner and localizer of BRCA2; RAD51B, RAD51 recombinase paralog B; WRN, WRN RecQ like helicase.

Table II. Classification of genetic variants in cholangiocarcinoma cell lines according to AMP guidelines.

	AMP classification, tier			
Genes	TFK-1	HuH-28	SiSP-K01	SiSP-K05
ARID1A	-	3	3	3
ARID1B	-	3	NA	NA
ATM	4	4	NA	-
ATR	4	4	3	3
ATRX	-	4	3	3
BAP1	3	-	-	-
BARD1	4	4	NA	-
BLM	-	3 and 4	-	3
BRCA1	-	-	2 and 3	NA
BRCA2	4	4	2 and 3	2 and 3
BRIP1	4	4	-	2 and 3
CHEK2	-	-	-	NA
FANCA	4	4	-	3
FANCF	-	-	-	3
PALB2	3	-	2 and 3	2
RAD50	-	-	-	NA
RAD51B	-	-	3	3
WRN	4	4	4	3

AMP, Association for Molecular Pathology; NA, not classifiable.

Drug combinations accelerate DNA damage as indicated by micronuclei and γ-H2AX formation. To determine whether combining AZD6738 with PARP inhibitors increases DNA damage compared with the individual effect of each drug at its IC_{50a}, micronuclei formation was evaluated in the CCA cell lines subjected to these treatments. The results showed that the drug combinations induced more DNA damage than each drug did on its own, particularly when cells were treated with the olaparib (Fig. 3A) and talazoparib (Fig. 3C) combinations. Specifically, in the case of olaparib (Fig. 3A), there were significant differences in the extent of damage when MMNK-1, TFK-1, SiSP-K01 and SiSP-K05 cell lines were treated with the combination of olaparib and AZD6738 compared with olaparib alone. For the TFK-1 cell line, a significant difference was also observed when the effect of combination treatment was compared with that of AZD6738 alone. With talazoparib (Fig. 3C), the SiSP-K01 cell line exhibited a significantly higher average number of micronuclei per cell when treated with the combination than with individual AZD6738 or talazoparib treatments. By contrast, SiSP-K05 presented a significant increase only when the combination was compared with talazoparib alone; no such increase was observed when compared with AZD6738 alone. However, in the context of veliparib (Fig. 3B), combining AZD6738 with veliparib did not result in a significant increase in micronuclei across all cell lines tested, with the exception of the SiSP-K01 cell line, in which a significant difference was found between the combination treatment and veliparib alone. Representative images of micronuclei for each condition are presented in Figs. S2-4.

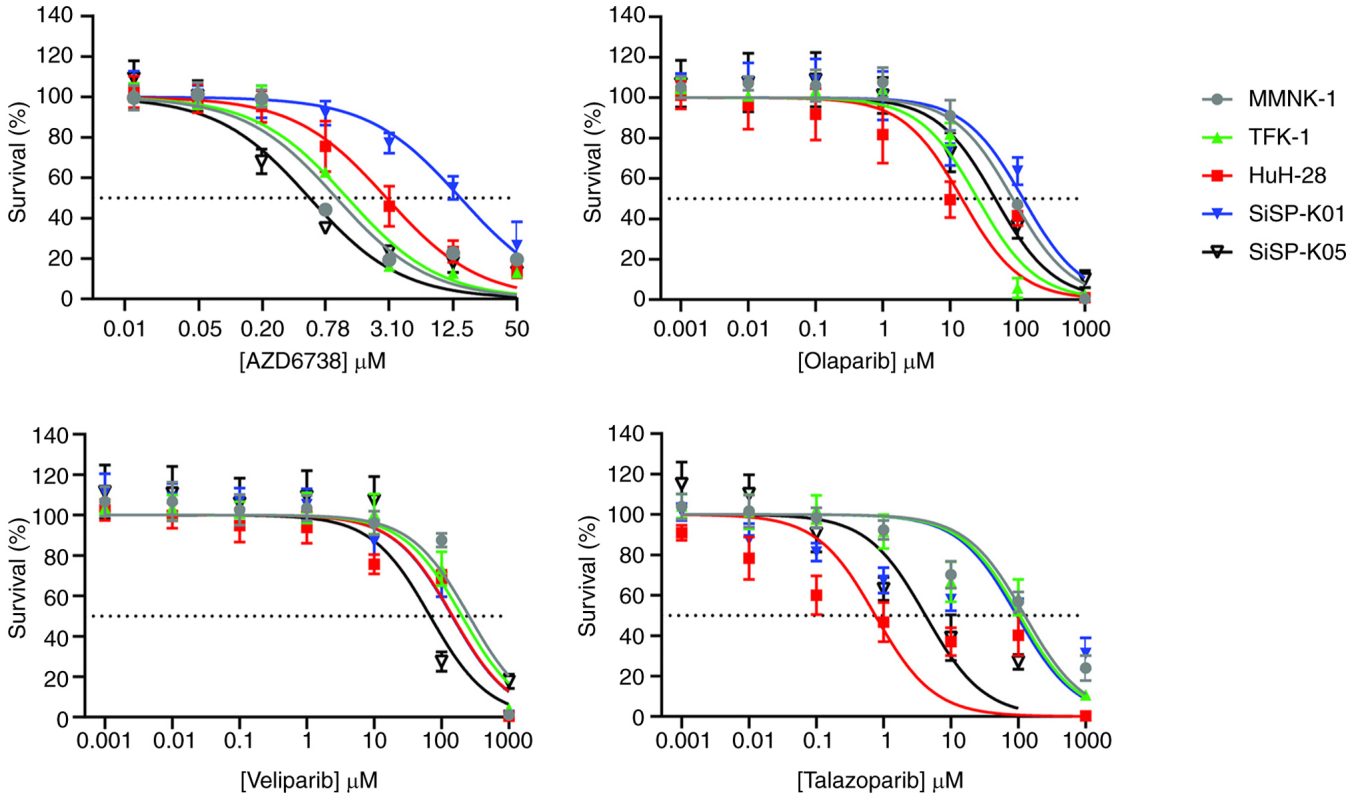

Figure 2. Dose-response curves from survival assays of cholangiocarcinoma and cholangiocyte cell lines treated with AZD6738 or various poly(ADP-ribose) polymerase inhibitors. The dashed line represents 50% survival.

The investigation was expanded to determine if the increased DNA damage seen following treatment with drug combinations could be attributed to a rise in DNA double-strand breaks, as compared with the individual effects of the drugs at their IC_{50a} (Fig. 4). The number of cell lines with significant increases in γ-H2AX foci, a marker of DNA double-strand breaks, following combination treatments when compared with AZD6738 alone was greater than that when compared with PARP inhibitor alone. Specifically, with olaparib and talazoparib (Fig. 4A and C), a significant increase in γ-H2AX foci was observed in all CCA cell lines and in normal cholangiocytes when these were compared with the effects of AZD6738 alone. However, with veliparib, the significant increase was noted only in CCA cell lines, not in cholangiocytes. Furthermore, the CCA cell lines HuH-28, SiSP-K01 and SiSP-K05 exhibited a significant increase in γ-H2AX when treated with combinations of olaparib or talazoparib, compared with these PARP inhibitors alone. With regard to veliparib, two CCA cell lines, HuH-28 and SiSP-K05, demonstrated a significant increase in γ-H2AX for the combination compared with veliparib alone. Representative images of γ-H2AX foci formation, indicative of DNA damage, are presented in Figs. S5-7.

These observations highlight the enhanced efficacy of combination treatments in inducing DNA damage, as compared with the effects of individual drug treatments. The pronounced increase in DNA double-strand breaks observed across various cell lines suggests the potential for synergistic interactions between AZD6738 and the PARP inhibitors.

Evaluating the impacts of AZD6738 and PARP inhibitor combinations on cell viability and CI. The effects of combinations of AZD6738 and different PARP inhibitors on cell viability were investigated, to determine which combinations yielded synergistic effects and dose reductions. The CI, a quantitative tool, was used to assess whether the drug interactions were synergistic, antagonistic or additive (36). First, the IC_{50c} profile of AZD6738 when combined with the PARP inhibitors olaparib, veliparib and talazoparib was determined as shown in Table IV, and the dose-response curves are presented in Fig. S8. Following this, the CIs were calculated, which are presented in Table V and visualized in Fig. 5.

The data reveal that all drug combinations were most effective against the SiSP-K05 cell line, with the IC_{50c} for each drug combination being lower for SiSP-K05 cells than for MMNK1 cells, as detailed in Table IV. Specifically, the combinations of AZD6738 with olaparib, veliparib and talazoparib consistently showed lower IC_{50c} values in SiSP-K05 cells compared with MMNK-1 cells. AZD6738 and olaparib had the following IC_{50c} values: MMNK-1, 1.238±0.083 and 1.655±0.161 μM; SiSP-K05, 0.641±0.116 μM (P=0.003) and 0.538±0.106 μM (P=0.002), respectively. For AZD6738 and veliparib, the IC_{50c} values were: MMNK-1, 1.307±0.118 and 1.438±0.179 μM; SiSP-K05, 0.612±0.103 μM (P=0.003) and 0.495±0.132 μM (P=0.002), respectively. AZD6738 and talazoparib had the following IC_{50c} values; MMNK-1, 1.178±0.084 and 0.633±0.090 μM; SiSP-K05, 0.319±0.007 μM (P<0.001) and 0.158±0.009 μM (P=0.002), respectively. By contrast, the SiSP-K01 cell line exhibited lower sensitivity than MMNK-1 cells to all these drug combinations, with IC_{50c} values as follows: AZD6738 and

Table III. IC_{50a} profiles from the sensitivity assay of cholangiocarcinoma and cholangiocyte cell lines in response to AZD6738 or various poly(ADP-ribose) polymerase inhibitors.

Drug	Cell line	IC_{50a}, μM	P-value
AZD6738	MMNK-1	0.997±0.141	-
	TFK-1	1.263±0.073	0.126
	HuH-28	3.204±1.587	0.074
	SiSP-K01	15.633±5.324	0.018
	SiSP-K05	0.554±0.020	0.017
Olaparib	MMNK-1	85.033±5.664	-
	TFK-1	25.667±3.661	<0.001
	HuH-28	19.740±16.283	0.010
	SiSP-K01	121.067±5.140	0.005
	SiSP-K05	46.790±16.939	0.021
Veliparib	MMNK-1	256.800±14.127	-
	TFK-1	202.067±47.561	0.241
	HuH-28	145.950±10.112	0.010
	SiSP-K01	143.833±20.857	0.005
	SiSP-K05	67.607±3.466	<0.001
Talazoparib	MMNK-1	127.767±39.302	-
	TFK-1	105.880±60.491	0.627
	HuH-28	1.095±0.920	0.010
	SiSP-K01	100.003±35.553	0.416
	SiSP-K05	4.378±1.977	0.017

IC_{50a} values are presented as the mean ± standard deviation. P-values are for the difference in IC_{50a} values vs. those of the respective drug in MMNK-1 cholangiocytes. IC_{50a}, half maximal inhibitory concentration of the drug used alone.

olaparib, 5.804±1.415 μM (P=0.005) and 33.953±17.481 μM (P=0.033); AZD6738 and veliparib; 6.802±0.172 μM (P<0.001) and 46.230±2.546 μM (P<0.001); AZD6738 and talazoparib; 2.703±0.373 μM (P=0.005) and 9.195±1.692 μM (P=0.002), respectively. Furthermore, HuH-28 cells were less sensitive than MMNK-1 cells to the combination of AZD6738 and veliparib, but both cell lines displayed a similar response to the combination of AZD6738 and olaparib. For the AZD6738 and talazoparib combination, the IC_{50c} of AZD6738 for both TFK-1 and HuH-28 cells differed significantly from that for MMNK-1 cells. However, no such difference was observed for talazoparib between these two cell lines. Notably, the IC_{50c} values for all PARP inhibitors were considerably lower when used in combination than when administered alone.

The CI analysis (Table V), revealed that synergistic effects were more prevalent in CCA cell lines when AZD6738 was combined with either olaparib or talazoparib, in comparison to its combination with veliparib. These findings are visually represented in Fig. 5. Specifically, the combination of AZD6738 and olaparib displayed synergistic effects in TFK-1, HuH-28 and SiSP-K01 cell lines. These effects varied, with values ranging from 0.623±0.097 in HuH-28 cells to 0.887±0.047 in TFK-1 cells. The combination of AZD6738 and talazoparib produced even stronger synergistic effects, with values spanning from 0.283±0.079 in SiSP-K01 cells to 0.619±0.051 in SiSP-K05 cells. Notably, the combinations comprising AZD6738 with either olaparib or talazoparib both showed synergistic effects in TFK-1 and SiSP-K01 cells. However, synergism in the SiSP-K05 cell line was only observed for the AZD6738 and talazoparib combination. Notably, all tested combinations exhibited synergistic effects in the SiSP-K01 cell line, with particularly strong synergism observed for the AZD6738 and talazoparib combination.

Overall, while synergistic effects were observed in SiSP-K01 cells for all drug combinations, the IC_{50c} profile indicates potential toxicity from these combinations. By contrast, the combination of AZD6738 and talazoparib appears to offer better efficacy for SiSP-K05 cells. This is evidenced by the IC_{50c} values of AZD6738 and talazoparib in SiSP-K05 cells being lower than those in MMNK-1 cells, and the observed synergistic effect of this combination.

Discussion

Since the first PARP inhibitor was approved by the FDA for the treatment of germline *BRCA* mutated advanced ovarian cancer, its indications have expanded to other types of cancers (11,41,42). Additionally, numerous ATR inhibitors have entered clinical trials, aiming to target replication stress and combat PARP inhibitor resistance (43). Currently, clinical trials are evaluating the treatment of various cancers with ATR inhibitors, particularly in combination with PARP inhibitors (44,45). However, only one ongoing trial is specifically addressing advanced CCA, focusing on the combination of AZD6738 and olaparib (24). The decreasing cost of sequencing has enabled more extensive genetic profiling to be performed in numerous types of cancer. This has increased research into how DDR-mutated profiles influence sensitivity to DNA damage and the response to repair-targeted drugs. In this context, the present study examined the response of cell lines with different DDR-mutated profiles to the ATR inhibitor AZD6738, various PARP inhibitors and their combinations. The results suggest that cell lines with a higher number of DDR mutations are more sensitive to AZD6738, PARP inhibitors and their combinations. Notably, among the PARP inhibitors, talazoparib exhibited the highest potency, both as a standalone treatment and in combination with AZD6738, for the treatment of CCA cell lines. Furthermore, combining PARP inhibitors with AZD6738 may reduce the toxicity associated with higher concentrations of ATR and PARP inhibitors.

It has been reported that alterations in DDR genes can be identified in up to 20% of patients with CCA, with extrahepatic CCA exhibiting a higher incidence than other CCA types (7). Several studies have investigated these alterations in CCA genes to expand the therapeutic use of ATR and PARP inhibitors. For example, a study by Bezrookove *et al* (26) analyzed the mutational profiles of DDR genes in 195 CCA samples using cBioPortal. They discovered that mutations in *ARID1A*, *BAP1* and *ATM* genes were particularly prevalent, being found in 20.51, 13.3 and 7.7% of cases, respectively. Based on these findings, the authors used four cell lines with different DDR mutation profiles to evaluate the response to the PARP inhibitors niraparib and olaparib. Niraparib inhibited cell growth more effectively than olaparib, but the response varied

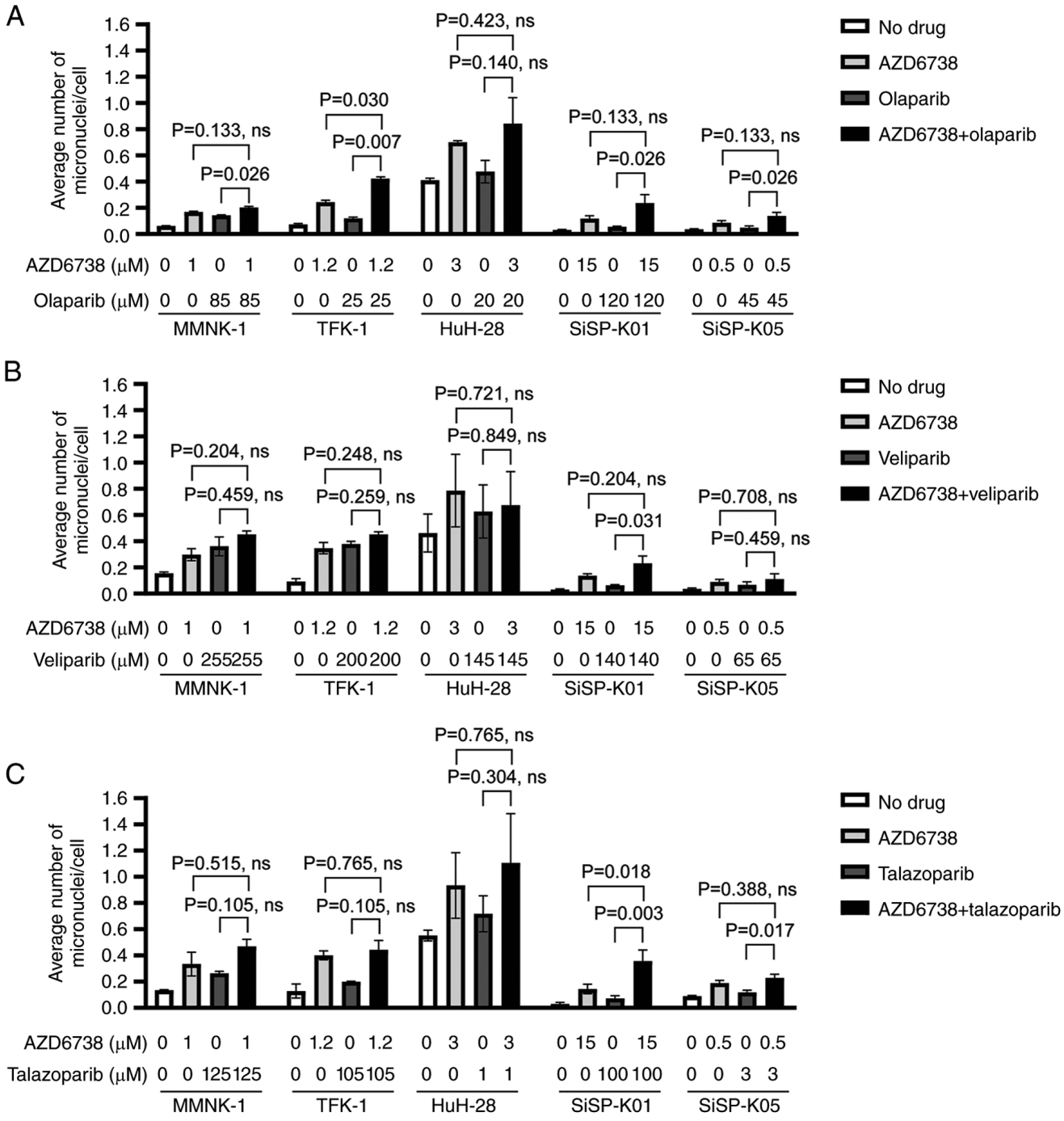

Figure 3. Micronuclei accumulation in cholangiocarcinoma and cholangiocyte cell lines following exposure to individual PARP inhibitors, AZD6738 or their combinations. The PARP inhibitors are (A) olaparib, (B) veliparib and (C) talazoparib. Controls for each drug group consisted of DMSO concentrations corresponding to those used in the drug combinations, which were (A) 0.026-0.451%, (B) 0.151-0.651% and (C) 0.007-0.252%; PARP, poly(ADP-ribose) polymerase; ns, no significant difference.

according to the mutational profile. In addition, a study by Serra-Camprubí *et al* (25) tested tumoroids derived from PDXs with confirmed pathogenic mutations in *ARID1A*, *BAP1* or *BRCA2* for sensitivity to olaparib, pamiparib and niraparib. The study revealed that tumoroids with a *BRCA2* defect exhibited sensitivity to olaparib and pamiparib, while other tumoroids did not respond to these PARP inhibitors. By comparison, the results of the present study indicate that mutations in *ATR*, *BRCA2* and *WRN* were present in all four CCA cell lines, while *ARID1A*, *ARID1B* and *ATRX* mutations were found in HuH-28, SiSP-K01 and SiSP-K05, and *ATM* mutations in TFK-1, HuH-28 and SiSP-K01. Among the tier 2 genes identified, *BRCA1*, *BRCA2* and *PALB2* have been reviewed by an expert panel in ClinVar (https://www.ncbi.nlm.nih.gov/clinvar/, accessed on September 15, 2023). However, only certain variants in *BRCA1* and *BRCA2* were acknowledged by the panel, while *PALB2* variants were not. Notably, the SiSP-K05 cell line, in which 15 mutated genes were detected, exhibited high sensitivity to both ATR and PARP inhibitors. While SiSP-K01 and HuH-28 were found

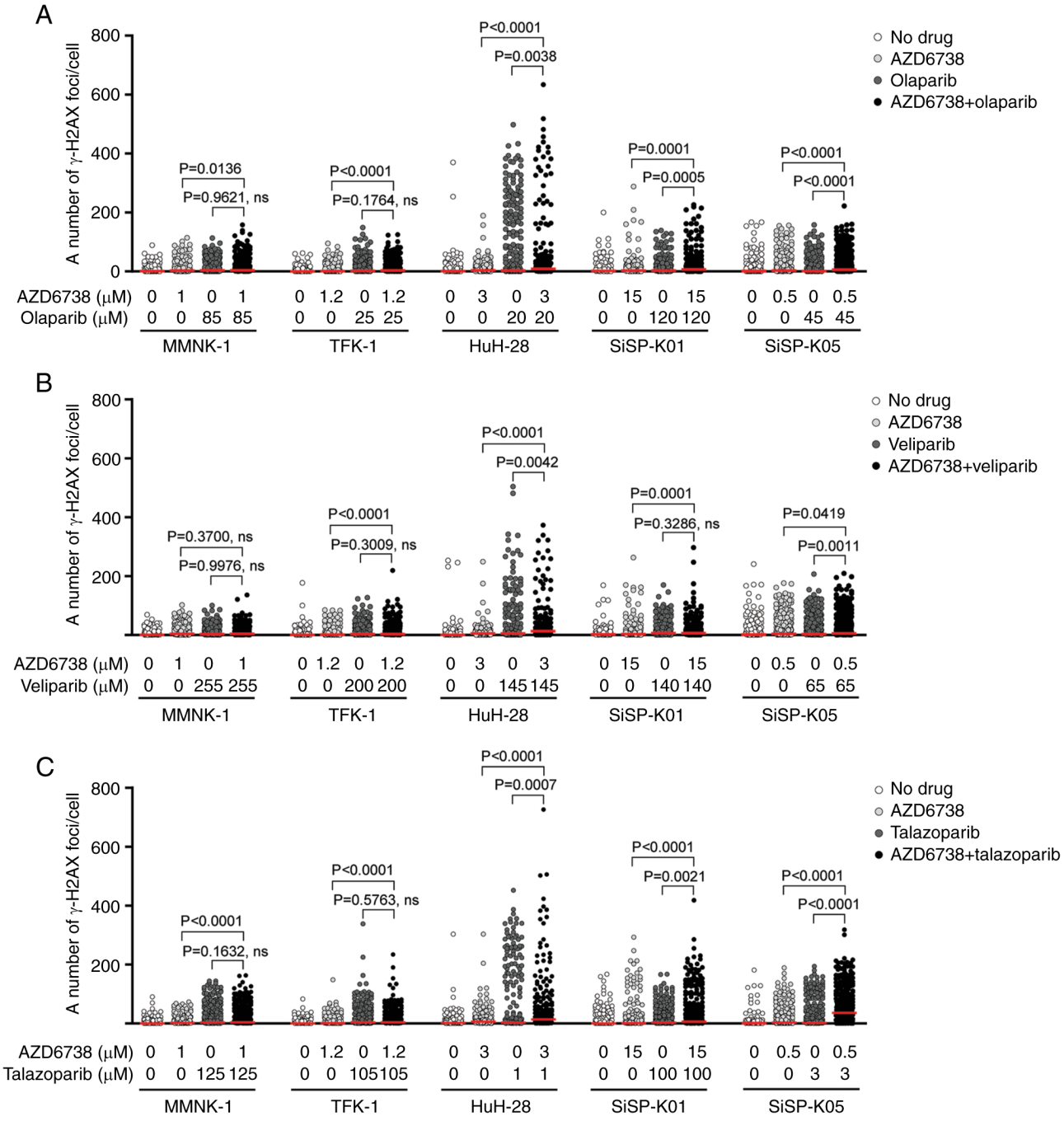

Figure 4. Levels of DNA damage as indicated by the number of g-H2AX foci/cell. Cholangiocarcinoma and cholangiocyte cell lines were treated with AZD6738, the poly(ADP-ribose) polymerase inhibitors (A) olaparib, (B) veliparib, (C) talazoparib, and their combinations. Controls for each drug group consisted of DMSO concentrations corresponding to those used in the drug combinations, which were (A) 0.026-0.451%, (B) 0.151-0.651% and (C) 0.007-0.252%. Red lines represent the median value. γ-H2AX, γ-H2A histone family member X; ns, no significant difference.

to share the same number of mutated genes (n=11), they displayed contrasting sensitivity profiles. SiSP-K01 exhibited low sensitivity, whereas the sensitivity pattern of HuH-28 was found to be similar to that of SiSP-K05. Notably, the only mutated gene exclusively shared between HuH-28 and SiSP-K05 is *BLM*, which could potentially contribute to the increased sensitivity of these cell lines to PARP and ATR inhibitors. This observation warrants further investigation. These findings suggest that an accumulation of mutations in DDR genes could potentially be a more accurate predictor of CCA sensitivity to PARP inhibitors than a single gene.

Targeting ATR has become an attractive therapeutic strategy since it was observed that cancer cells are vulnerable to replication stress (46). This finding has been supported by studies focusing on CCA cell lines. Nam *et al* (47) investigated the response to AZD6738 of nine CCA cell lines with varying expression levels of ATR, ATM and p53. Their findings revealed that cell lines with low levels of both ATM and p53 were sensitive to AZD6738, while those with low ATM but high p53 levels exhibited resistance. In another study, Moolmuang and Ruchirawat (27) reported the sensitivity of three CCA cell lines to the ATR inhibitor

Table IV. IC_{50c} profiles of cholangiocarcinoma and cholangiocyte cell lines in response to various combinations of AZD6738 and PARP inhibitors.

		AZD6738		PARP inhibitor	
Drug combination	Cell line	IC_{50c}, μM	P-value[a]	IC_{50c}, μM	P-value[a]
AZD6738 + olaparib	MMNK-1	1.238±0.083	-	1.655±0.161	-
	TFK-1	1.043±0.070	0.070	1.540±0.133	0.394
	HuH-28	1.417±0.590	0.630	2.699±1.611	0.327
	SiSP-K01	5.804±1.415	0.005	33.953±17.481	0.033
	SiSP-K05	0.641±0.116	0.003	0.538±0.106	0.002
AZD6738 + veliparib	MMNK-1	1.307±0.118	-	1.438±0.179	-
	TFK-1	1.51±0.419	0.462	2.625±1.033	0.228
	HuH-28	2.377±0.122	0.004	6.104±0.599	0.003
	SiSP-K01	6.802±0.172	<0.001	46.230±2.546	<0.001
	SiSP-K05	0.612±0.103	0.003	0.495±0.132	0.002
AZD6738 + talazoparib	MMNK-1	1.178±0.084	-	0.633±0.090	-
	TFK-1	0.501±0.031	<0.001	0.425±0.030	0.056
	HuH-28	0.451±0.098	0.002	0.424±0.167	0.241
	SiSP-K01	2.703±0.373	0.005	9.195±1.692	0.002
	SiSP-K05	0.319±0.007	<0.001	0.158±0.009	0.002

IC_{50c} values are presented as the mean ± standard deviation. [a]P-values are for the difference in IC_{50c} values vs. those of the respective drug in MMNK-1 cholangiocytes. IC_{50c}, half maximal concentration of each drug used in combination; PARP, poly(ADP-ribose) polymerase.

Table V. CI values of various combinations of AZD6738 and poly(ADP-ribose) polymerase inhibitors.

Drug combination	Cell line	CI
AZD6738 + olaparib	MMNK-1	1.269±0.091
	TFK-1	0.887±0.047
	HuH-28	0.623±0.097
	SiSP-K01	0.659±0.092
	SiSP-K05	1.167±0.185
AZD6738 + veliparib	MMNK-1	1.323±0.094
	TFK-1	1.200±0.280
	HuH-28	1.182±0.709
	SiSP-K01	0.804±0.126
	SiSP-K05	1.109±0.153
AZD6738 + talazoparib	MMNK-1	1.195±0.094
	TFK-1	0.403±0.015
	HuH-28	1.007±0.736
	SiSP-K01	0.283±0.079
	SiSP-K05	0.619±0.051

CI, combination index.

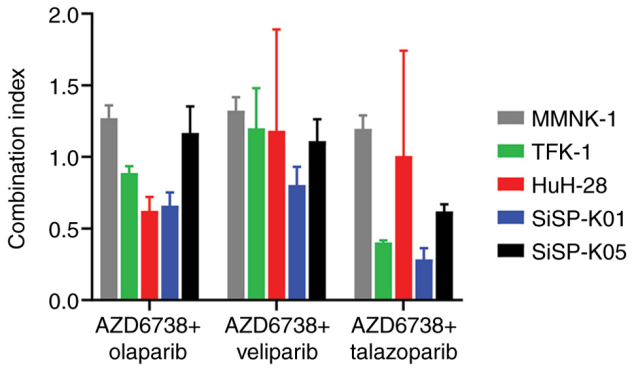

Figure 5. Combination index values in cholangiocarcinoma and cholangiocyte cell lines of the indicated combination treatments.

VE-821. The study highlighted the effectiveness of VE-821 in inhibiting the colony formation of CCA cells, but it did not provide information on DDR-related molecular profiles that might explain the varying drug responses. By comparison, in the present study, only the SiSP-K05 cell line showed a high sensitivity to AZD6738. SiSP-K01 was less sensitive, with an IC_{50a} value >10 mM, which was higher than that in MMNK-1 cells. Several studies have suggested that the level of replicative stress contributes to the sensitivity towards ATR inhibitors. For instance, Dorado Garcia *et al* (48) demonstrated that increased replicative stress in paired box 3-forkhead box O1-expressing alveolar rhabdomyosarcoma cells heightened their sensitivity to ATR inhibitors. In addition, a study by King *et al* (49) showed that high-risk neuroblastomas with MYCN proto-oncogene-induced replication stress are highly susceptible to ATR inhibitors VE-821 and AZD6738. Consequently, the lower sensitivity of SiSP-K01 to AZD6738 may be associated with reduced levels of replicative stress. However, it is hypothesized that CCA cells can develop resistance to ATR inhibitors if the replicative stress is mitigated by other pathways, potentially decreasing treatment efficacy. Further investigation is warranted to confirm this notion.

To enhance the efficacy of PARP inhibitors and prevent resistance to these drugs, combining PARP inhibitors with ATR inhibitors has been proposed as a promising treatment strategy for several types of cancer, such as ovarian and prostate cancer (50). Furthermore, numerous clinical trials are actively recruiting patients to assess the effectiveness of ATR inhibitors in combination with various PARP inhibitors (51). It has been shown that this type of combination results in increased DNA damage, leading to mitotic catastrophe and p53-independent cell death (48). This DNA damage can be assessed using micronuclei and comet assays as indicators of genomic instability, with the detection of γ-H2AX formation to indicate DNA double-strand break formation (52). Nam *et al* (28) demonstrated that the combination of AZD6738 and olaparib induced greater DNA damage in CCA cell lines than either drug alone, as evidenced by a comet assay. Similarly, King *et al* (49) observed increased DNA damage in high-risk neuroblastomas treated with a combination of VE-821 and olaparib. In addition, a study performed by Sule *et al* (53) revealed that the combination of AZD6738 and olaparib induced DNA damage in IDH1-mutant cell lines, as shown by the increased formation of γ-H2AX. Lloyd *et al* (54) demonstrated that a similar combination promoted genomic instability in ATM-defective cell lines, identified through micronuclei analysis. In the present study, the results regarding micronuclei and γ-H2AX formation align with these findings, demonstrating a similar pattern of increased micronuclei formation and γ-H2AX levels, particularly in cases where AZD6738 is combined with either olaparib or talazoparib. Notably, these combinations resulted in more extensive damage compared with the effects of the drugs used individually. However, it is crucial to consider that several mechanisms, beyond ATR activation, can contribute to PARP inhibitor resistance in CCA. These include the restoration of HR, mutations in PARP that diminish PARP inhibitor binding, and increased PARP inhibitor efflux (55). Further studies are required to explore these possibilities in CCA, in order to optimize treatment strategies and minimize the development of resistance.

In clinical practice, toxicity must be considered, as a combinational approach could potentially produce severe effects, particularly with drugs targeting DDR pathways (42). Conducting preclinical drug combination studies to understand drug interactions through the CI can be rational for studies in humans (35). The results of the present demonstrate that combination regimens have the potential to reduce the required dose of PARP inhibitors from that used as a monotherapy. The combination of AZD6738 and talazoparib resulted in a stronger synergistic effect compared with other combinations, particularly in TFK-1, SiSP-K01 and SiSP-K05 cell lines. Olaparib and talazoparib, both FDA-approved for several types of cancer, differ in their mechanisms; talazoparib is more potent than olaparib in PARP-trapping, which refers to the process of retaining the PARP-DNA complex, thus enhancing the cytotoxicity of talazoparib (56,57). Previous studies have demonstrated that the proteins responding to PARP-trapping differ from those responding to non-trapping PARP inhibitors, and these responses vary depending on the type of cancer (58,59). This may explain why synergistic effects were observed to vary in CCA cell lines with different molecular backgrounds.

The strength of the present study is the elucidation of the relationship between DDR-mutated profiles and the response to AZD6738, various PARP inhibitors, and their combinations. The study also discovered that the number of mutated genes contributes to the response to individual drugs and their combinations. However, it should be noted that while some combinations exhibited an improved CI, the concentrations used were still toxic to normal cells. Therefore, the development of a targeted drug delivery system for this type of CCA may enhance treatment efficacy. Alternatively, pre-selecting cancers that are more vulnerable to these drug combinations, for example, by the measurement of replicative stress, could reduce drug toxicity.

A limitation of the present study is the limited number of cell lines used, considering that CCA is heterogeneous, and its mutational profiles vary depending on etiological agents and tumor locations. Therefore, more diverse cell lines are required to confirm if the accumulation of certain DDR genes benefits from ATR and PARP inhibitors, either alone or in combination. Additionally, while genetic profiling was used, functional biomarkers such as DNA fiber assays or RAD51 foci formation were not included. These could provide more insight and serve as additional criteria for determining the sensitivity to DDR inhibitors. Moreover, the frequency of genetic variations in the CCA cell lines was not well established, leaving to uncertainty about which mutations are predominant in these cell lines. The study also lacks evaluation of the long-term treatment of CCA using dose-escalating protocols for a defined duration, for example, starting with a low dose for 3 months, escalating to a higher dose for another 6 months and then using a maintenance dose for 9 months. Such evaluation would provide an increased understanding of the dynamics of genetic alterations associated with the development of drug resistance. Finally, future research should include *in vivo* validation experiments in animal models, such as PDX and pharmacokinetic studies. This would enable evaluation of the complex tumor microenvironment and its impact on drug response, including drug toxicity.

Acknowledgements

The authors would like to thank Professor Seiji Okada (Division of Hematopoiesis, Joint Research Center for Human Retrovirus Infection & Graduate School of Medical Sciences, Kumamoto University, Kumamoto, Japan) for experimental support.

Funding

This research is supported by Mahidol University (Basic Research Fund: fiscal year 2022) and the National Research Council of Thailand (grant no. N41A640160). SJ is supported by the National Research Council of Thailand (grant no. N41A640162) and the Foundation for Cancer Care Siriraj Hospital.

Availability of data and materials

The next-generation sequencing results generated for SiSP-K01 and SiSP-K05 in the present study may be found in the Sequence Read Archive at the following URLs (https://www.ncbi.nlm.nih.gov/sra/SRR31111387 and https://www.ncbi.nlm.nih.gov/sra/SRR31111386). The other data generated in

the present study may be requested from the corresponding authors.

Authors' contributions

TL contributed to data interpretation, formal analysis, experimentation, methodology and visualization, and wrote the original draft of the manuscript. SP and RW contributed to methodology, experimentation and manuscript review and editing. SC, WS and PO contributed to the experimentation, and participated in the review and editing of the manuscript. SJ was responsible for conceptualization, resource and funding acquisition, and contributed to manuscript review and editing. DD supervised the study, and contributed to conceptualization, funding acquisition and manuscript review and editing. DD and SJ confirm the authenticity of all the raw data. All authors read and approved the final version of the manuscript.

Ethics approval and consent to participate

The protocol was approved by the Human Research Ethics Committee, Faculty of Medicine Ramathibodi Hospital, Mahidol University (Bangkok, Thailand; approval no. MURA2023/155). The study utilized established primary cell lines obtained from Professor Seiji Okada, Kumamoto University (Kumamoto, Japan) and handled in accordance with the guidelines and regulations of the Human Research Ethics Committee of Ramathibodi Hospital.

Patient consent for publication

Not applicable.

Competing interests

The authors declare that they have no competing interests.

Use of artificial intelligence tools

During the preparation of this work, ChatGPT 4 was utilized for spelling and grammar checks. Subsequently, the authors reviewed and edited the content as necessary, taking full responsibility for the ultimate content of the present manuscript.

References

1. Brindley PJ, Bachini M, Ilyas SI, Khan SA, Loukas A, Sirica AE, The BT, Wongkham S and Gores GJ: Cholangiocarcinoma. Nat Rev Dis Primers 7: 65, 2021.
2. Banales JM, Marin JJG, Lamarca A, Rodrigues PM, Khan SA, Roberts LR, Cardinale V, Carpino G, Andersen JB, Braconi C, *et al*: Cholangiocarcinoma 2020: The next horizon in mechanisms and management. Nat Rev Gastroenterol Hepatol 17: 557-588, 2020.
3. Ohaegbulam KC, Koethe Y, Fung A, Mayo SC, Grossberg AJ, Chen EY, Sharzehi K, Kardosh A, Farsad K, Rocha FG, *et al*: The multidisciplinary management of cholangiocarcinoma. Cancer 129: 184-214, 2023.
4. Squadroni M, Tondulli L, Gatta G, Mosconi S, Beretta G and Labianca R: Cholangiocarcinoma. Crit Rev Oncol Hematol 116: 11-31, 2017.
5. Gönül Geyik Ö, Anichini G, Ulukaya E, Marra F and Raggi C: DNA damage response inhibitors in cholangiocarcinoma: Current progress and perspectives. Cells 11: 1463, 2022.
6. Chae H, Kim D, Yoo C, Kim KP, Jeong JH, Chang HM, Lee SS, Park DH, Song TJ, Hwang S, *et al*: Therapeutic relevance of targeted sequencing in management of patients with advanced biliary tract cancer: DNA damage repair gene mutations as a predictive biomarker. Eur J Cancer 120: 31-39, 2019.
7. Ahn DH and Bekaii-Saab T: Biliary tract cancer and genomic alterations in homologous recombinant deficiency: Exploiting synthetic lethality with PARP inhibitors. Chin Clin Oncol 9: 6, 2020.
8. Beijersbergen RL, Wessels LFA and Bernards R: Synthetic lethality in cancer therapeutics. Annu Rev Cancer Biol 1: 141-161, 2017.
9. Pilié PG, Tang C, Mills GB and Yap TA: State-of-the-art strategies for targeting the DNA damage response in cancer. Nat Rev Clin Oncol 16: 81-104, 2019.
10. D'Andrea AD: Mechanisms of PARP inhibitor sensitivity and resistance. DNA Repair (Amst) 71: 172-176, 2018.
11. Fong PC, Boss DS, Yap TA, Tutt A, Wu P, Mergui-Roelvink M, Mortimer P, Swaisland H, Lau A, O'Connor MJ, *et al*: Inhibition of poly(ADP-ribose) polymerase in tumors from BRCA mutation carriers. N Engl J Med 361: 123-134, 2009.
12. Balasubramaniam S, Beaver JA, Horton S, Fernandes LL, Tang S, Horne HN, Liu J, Liu C, Schrieber SJ, Yu J, *et al*: FDA approval summary: rucaparib for the treatment of patients with deleterious BRCA mutation-associated advanced ovarian cancer. Clin Cancer Res 23: 7165-7170, 2017.
13. Mirza MR, Monk BJ, Herrstedt J, Oza AM, Mahner S, Redondo A, Fabbro M, Ledermann JA, Lorusso D, Vergote I, *et al*: Niraparib maintenance therapy in platinum-sensitive, recurrent ovarian cancer. N Engl J Med 375: 2154-2164, 2016.
14. Hoy SM: Talazoparib: First global approval. Drugs 78: 1939-1946, 2018.
15. Li N, Bu H, Liu J, Zhu J, Zhou Q, Wang L, Yin R, Wu X, Yao S, Gu K, *et al*: An open-label, multicenter, single-arm, phase II study of fluzoparib in patients with germline BRCA1/2 mutation and platinum-sensitive recurrent ovarian cancer. Clin Cancer Res 27: 2452-2458, 2021.
16. Xu B, Yin Y, Dong M, Song Y, Li W, Huang X, Wang T, He J, Mu X, Li L, *et al*: Pamiparib dose escalation in Chinese patients with non-mucinous high-grade ovarian cancer or advanced triple-negative breast cancer. Cancer Med 10: 109-118, 2021.
17. da Costa AABA, Chowdhury D, Shapiro GI, D'Andrea AD and Konstantinopoulos PA: Targeting replication stress in cancer therapy. Nat Rev Drug Discov 22: 38-58, 2023.
18. Smith G, Alholm Z, Coleman RL and Monk BJ: DNA damage repair inhibitors-combination therapies. Cancer J 27: 501-505, 2021.
19. Mullard A: DNA damage response drugs for cancer yield continued synthetic lethality learnings. Nat Rev Drug Discov 21: 403-405, 2022.
20. Shah PD, Wethington SL, Pagan C, Latif N, Tanyi J, Martin LP, Morgan M, Burger RA, Haggerty A, Zarrin H, *et al*: Combination ATR and PARP inhibitor (CAPRI): A phase 2 study of ceralasertib plus olaparib in patients with recurrent, platinum-resistant epithelial ovarian cancer. Gynecol Oncol 163: 246-253, 2021.
21. Clinical Trials: NCT03330847: To assess safety and efficacy of agents targeting DNA damage repair with olaparib versus olaparib monotherapy. https://clinicaltrials.gov/show/NCT03330847. Accessed June 4, 2023.
22. Clinical Trials: NCT03787680: Targeting resistant prostate cancer with ATR and PARP inhibition (TRAP Trial). https://clinicaltrials.gov/show/NCT03787680. Accessed June 4, 2023.
23. Clinical Trials: NCT03878095: Testing olaparib and AZD6738 in IDH1 and IDH2 mutant tumors. https://clinicaltrials.gov/show/NCT03878095. Accessed June 4, 2023.
24. Clinical Trials: NCT04298021: DDR-umbrella study of DDR targeting agents in advanced biliary tract cancer. https://clinicaltrials.gov/study/NCT04298021. Accessed November 13, 2023.
25. Serra-Camprubí Q, Verdaguer H, Oliveros W, Lupión-Garcia N, Llop-Guevara A, Molina C, Vila-Casadesús M, Turpin A, Neuzillet C, Frigola J, *et al*: Human metastatic cholangiocarcinoma patient-derived xenografts and tumoroids for preclinical drug evaluation. Clin Cancer Res 29: 432-445, 2023.
26. Bezrookove V, Patino JM, Nosrati M, Desprez PY, McAllister S, Soroceanu L, Baron A, Osorio R, Kashani-Sabet M and Dar AA: Niraparib suppresses cholangiocarcinoma tumor growth by inducing oxidative and replication stress. Cancers (Basel) 13: 4405, 2021.
27. Moolmuang B and Ruchirawat M: The antiproliferative effects of ataxia-telangiectasia mutated and ATM- and Rad3-related inhibitions and their enhancements with the cytotoxicity of DNA damaging agents in cholangiocarcinoma cells. J Pharm Pharmacol 73: 40-51, 2021.

28. Nam AR, Yoon J, Jin MH, Bang JH, Oh KS, Seo HR, Kim JM, Kim TY and Oh DY: ATR inhibition amplifies antitumor effects of olaparib in biliary tract cancer. Cancer Lett 516: 38-47, 2021.
29. Maruyama M, Kobayashi N, Westerman KA, Sakaguchi M, Allain JE, Totsugawa T, Okitsu T, Fukazawa T, Weber A, Stolz DB, *et al*: Establishment of a highly differentiated immortalized human cholangiocyte cell line with SV40T and hTERT. Transplantation 77: 446-451, 2004.
30. Kusaka Y, Tokiwa T and Sato J: Establishment and characterization of a cell line from a human cholangiocellular carcinoma. Res Exp Med (Berl) 188: 367-375, 1988.
31. Saijyo S, Kudo T, Suzuki M, Katayose Y, Shinoda M, Muto T, Fukuhara K, Suzuki T and Matsuno S: Establishment of a new extrahepatic bile duct carcinoma cell line, TFK-1. Tohoku J Exp Med 177: 61-71, 1995.
32. Suntiparpluacha M, Chanwat R, Limsrichamrern S, More-krong P, Srifa S, Kongsri K Aroonpruksakul S, Sathirareuangchai S, Sampatavanich S, Okada S and Jirawatnotai S: Establishment of cholangiocarcinoma organoids from long-term frozen tissues. J Basic Appl Pharmacol 2: O11-O25, 2022.
33. Jamnongsong S, Kueanjinda P, Buraphat P, Sakornsakolpat P, Vaeteewoottacharn K, Okada S, Jirawatnotai S and Sampattavanich S: Comprehensive drug response profiling and pan-omic analysis identified therapeutic candidates and prognostic biomarkers for Asian cholangiocarcinoma. iScience 25: 105182, 2022.
34. Li MM, Datto M, Duncavage EJ, Kulkarni S, Lindeman NI, Roy S, Tsimberidou AM, Vnencak-Jones CL, Wolff DJ, Younes A and Nikiforova MN: Standards and guidelines for the interpretation and reporting of sequence variants in cancer: A joint consensus recommendation of the association for molecular pathology, American society of clinical oncology, and college of american pathologists. J Mol Diagn 19: 4-23, 2017.
35. Chou TC: Drug combination studies and their synergy quantification using the Chou-Talalay method. Cancer Res 70: 440-446, 2010.
36. Chou TC: Theoretical basis, experimental design, and computerized simulation of synergism and antagonism in drug combination studies. Pharmacol Rev 58: 621-681, 2006.
37. Schindelin J, Arganda-Carreras I, Frise E, Kaynig V, Longair M, Pietzsch T, Preibisch S, Rueden C, Saalfeld S, Schmid B, *et al*: Fiji: An open-source platform for biological-image analysis. Nat Methods 9: 676-682, 2012.
38. Jang SM, Redon CE, Fu H, Indig FE and Aladjem MI: RepID-deficient cancer cells are sensitized to a drug targeting p97/VCP segregase. Mol Cell Toxicol 17: 141-149, 2021.
39. Wikiniyadhanee R, Lerksuthirat T, Stitchantrakul W, Chitphuk S, Sura T and Dejsuphong D: TRIM29 is required for efficient recruitment of 53BP1 in response to DNA double-strand breaks in vertebrate cells. FEBS Open Bio 10: 2055-2071, 2020.
40. Lerksuthirat T, Wikiniyadhanee R, Chitphuk S, Stitchantrakul W, Sampattavanich S, Jirawatnotai S, Jumpathong J and Dejsuphong D: DNA Repair Biosensor-Identified DNA Damage Activities of Endophyte Extracts from *Garcinia* cowa. Biomolecules 10: 1680, 2020.
41. Audeh MW, Carmichael J, Penson RT, Friedlander M, Powell B, Bell-McGuinn KM, Scott C, Weitzel JN, Oaknin A, Loman N, *et al*: Oral poly(ADP-ribose) polymerase inhibitor olaparib in patients with BRCA1 or BRCA2 mutations and recurrent ovarian cancer: A proof-of-concept trial. Lancet 376: 245-251, 2010.
42. Martorana F, Da Silva LA, Sessa C and Colombo I: Everything comes with a price: The toxicity profile of DNA-damage response targeting agents. Cancers (Basel) 14: 953, 2022.
43. Bradbury A, Hall S, Curtin N and Drew Y: Targeting ATR as cancer therapy: A new era for synthetic lethality and synergistic combinations? Pharmacol Ther 207: 107450, 2020.
44. Clinical Trials: NCT03462342: Combination ATR and PARP inhibitor (CAPRI) trial with AZD6738 and olaparib in recurrent ovarian cancer (CAPRI). https://clinicaltrials.gov/study/NCT03462342. Accessed November 11, 2023.
45. Clinical Trials: NCT05269316: Study to evaluate IMP9064 as a monotherapy or in combination in patients with advanced solid tumors. https://www.clinicaltrials.gov/study/NCT05269316. Accessed November 11, 2023.
46. Lecona E and Fernandez-Capetillo O: Targeting ATR in cancer. Nat Rev Cancer 18: 586-595, 2018.
47. Nam AR, Jin MH, Park JE, Bang JH, Oh DY and Bang YJ: Therapeutic targeting of the DNA damage response using an ATR inhibitor in biliary tract cancer. Cancer Res Treat 51: 1167-1179, 2019.
48. Dorado Garcia H, Pusch F, Bei Y, von Stebut J, Ibáñez G, Guillan K, Imami K, Gürgen D, Rolff J, Helmsauer K, *et al*: Therapeutic targeting of ATR in alveolar rhabdomyosarcoma. Nat Commun 13: 4297, 2022.
49. King D, Southgate HED, Roetschke S, Gravells P, Fields L, Watson JB, Chen L, Chapman D, Harrison D, Yeomanson D, *et al*: Increased replication stress determines ATR inhibitor sensitivity in neuroblastoma cells. Cancers (Basel) 13: 6215, 2021.
50. Bhamidipati D, Haro-Silerio JI, Yap TA and Ngoi N: PARP inhibitors: Enhancing efficacy through rational combinations. Br J Cancer 129: 904-916, 2023.
51. Yano K and Shiotani B: Emerging strategies for cancer therapy by ATR inhibitors. Cancer Sci 114: 2709-2721, 2023.
52. Sadeghi F, Asgari M, Matloubi M, Ranjbar M, Karkhaneh Yousefi N, Azari T and Zaki-Dizaji M: Molecular contribution of BRCA1 and BRCA2 to genome instability in breast cancer patients: Review of radiosensitivity assays. Biol Proced Online 22: 23, 2020.
53. Sule A, Van Doorn J, Sundaram RK, Ganesa S, Vasquez Juan C and Bindra Ranjit S: Targeting IDH1/2 mutant cancers with combinations of ATR and PARP inhibitors. NAR Cancer 3: zcab018, 2021.
54. Lloyd RL, Wijnhoven PWG, Ramos-Montoya A, Wilson Z, Illuzzi G, Falenta K, Jones GN, James N, Chabbert CD, Stott J, *et al*: Combined PARP and ATR inhibition potentiates genome instability and cell death in ATM-deficient cancer cells. Oncogene 39: 4869-4883, 2020.
55. Lee EK and Matulonis UA: PARP inhibitor resistance mechanisms and implications for post-progression combination therapies. Cancers (Basel) 12: 2054, 2020.
56. Onji H and Murai J: Reconsidering the mechanisms of action of PARP inhibitors based on clinical outcomes. Cancer Sci 113: 2943-2951, 2022.
57. Murai J, Huang SYN, Renaud A, Zhang Y, Ji J, Takeda S, Morris J, Teicher B, Doroshow JH and Pommier Y: Stereospecific PARP trapping by BMN 673 and comparison with olaparib and rucaparib. Mol Cancer Ther 13: 433-443, 2014.
58. Mosler T, Baymaz HI, Gräf JF, Mikicic I, Blattner G, Bartlett E, Ostermaier M, Piccinno R, Yang J, Voigt A, *et al*: PARP1 proximity proteomics reveals interaction partners at stressed replication forks. Nucleic Acids Res 50: 11600-11618, 2022.
59. Zamalloa LG, Pruitt MM, Hermance NM, Gali H, Flynn RL and Manning AL: RB loss sensitizes cells to replication-associated DNA damage after PARP inhibition by trapping. Life Sci Alliance 6: e202302067, 2023.

Copyright © 2025 Lerksuthirat et al. This work is licensed under a Creative Commons Attribution-NonCommercial-NoDerivatives 4.0 International (CC BY-NC-ND 4.0) License.